

Simulations of thermal surface waves in a protoplanetary disk using 1+1D approximation

Ya. N. Pavlyuchenkov, L. A. Maksimova, V. V. Akimkin

Institute of Astronomy RAS, Moscow, Russia

Received 30.10.2021; revised 17.01.2022; accepted 24.01.2022

pavyar@inasan.ru

ABSTRACT

Heating by the central star is one of the key factors determining the physical structure of protoplanetary disks. Due to the large optical thickness in the radial direction, disk midplane regions are heated by the infrared radiation from the disk surface (atmosphere), which in turn is directly heated by the star. It was previously shown that interception of the stellar radiation by inhomogeneities on the disk surface can cause perturbations that propagate towards the star. In this work, we investigate the occurrence of such waves within a detailed 1+1D numerical model of the protoplanetary disk. We confirm the previous findings that in the disk, that is optically thick to its own radiation, the surface perturbations indeed occur and propagate towards the star. However, contrary to some analytical predictions, the thermal waves in sufficiently massive disks affect only the upper layers without significant fluctuations of temperature in the midplane. Our results indicate the need to study this instability within more consistent hydrodynamic models.

DOI: 10.31857/S000462992205005X

1 INTRODUCTION

Solving the problem of the formation of stars and planets is an important astrophysical and worldview challenge. However, despite the success in building a general pictures of stars and planets formation, details of the protoplanetary disks evolution (precursors of planetary systems) and the role of various physical processes have not yet been fully clarified. This is primarily due to the variety of physical processes in protoplanetary disks and their complex interaction. In protoplanetary disks, the conditions for occurrence of a wide variety of dynamic instabilities are satisfied. Their development can affect both the observational manifestations and the general disk evolution.

Recent observations made with the ALMA telescope array have shown that the disk surface density distributions do not correspond to smooth power laws often used by theorists. On the contrary, on the scale of tens to hundreds of au bright rings and dark gaps are common phenomena (ALMA Partnership et al. (2015); Andrews (2020); Huang et al. (2018)). For now, these rings and gaps are most often explained by the influence of invisible planets (Baruteau et al. (2014); Dong, Zhu & Whitney (2015); Dipierro et al. (2016); Bae, Zhu & Hartmann (2017); Zhang et al. (2018)). However, many alternative scenarios have been proposed to explain these features. One of them is the instability associated with the interception of stellar radiation by the surface inhomogeneities of the disk.

This instability (known as irradiation instability or thermal wave instability) can cause the emergence of surface waves traveling towards the star, and ring structures in circumstellar disks (D'Alessio et al. (1999); Dullemond (2000); Watanabe & Lin (2008); Siebenmorgen & Heymann (2012)). The mechanism of this

physical instability is as follows. If a small bump forms on the surface of the disk, then the illuminated side of the bump, facing the star, receives more starlight and heats up. The warm elements of the bump heat the lower layers of the disk with their radiation, as a result the formed bump grows. Since the side of the bump facing the star heats up more strongly than the opposite side, the perturbation also begins to move towards the star.

Recently, significant progress has been made in the study of this instability, see Ueda, Flock & Birnstiel (2021) and Wu & Lithwick (2021). In particular, in Wu & Lithwick (2021) within the framework of an analytical approximation, it is shown that this instability actually takes place. Moreover, the key role in the development of instability is the detailed account of dependence of H/h on the distance (where H is the optical height of the disk, and h is the characteristic hydrostatic scale height). In addition to the analytical model, the authors of Wu & Lithwick (2021) also presented semi-analytical model where the evolution of the midplane temperature is derived using the heating function calculated by the radiation transfer code RADMC-3D.

The purpose of this work is to study the irradiation instability within a more detailed numerical model of the protoplanetary disk, where the transfer of stellar radiation is treated in two-dimensional approach while the non-stationary thermal disk structure is calculated on the entire vertical scale of the disk.

2 QUASI-HYDROSTATIC 1+1D MODEL OF A PROTOPLANETARY DISK

To calculate the evolution of the disk, we adopt the model described in Vorobyov & Pavlyuchenkov (2017); Pavlyuchenkov

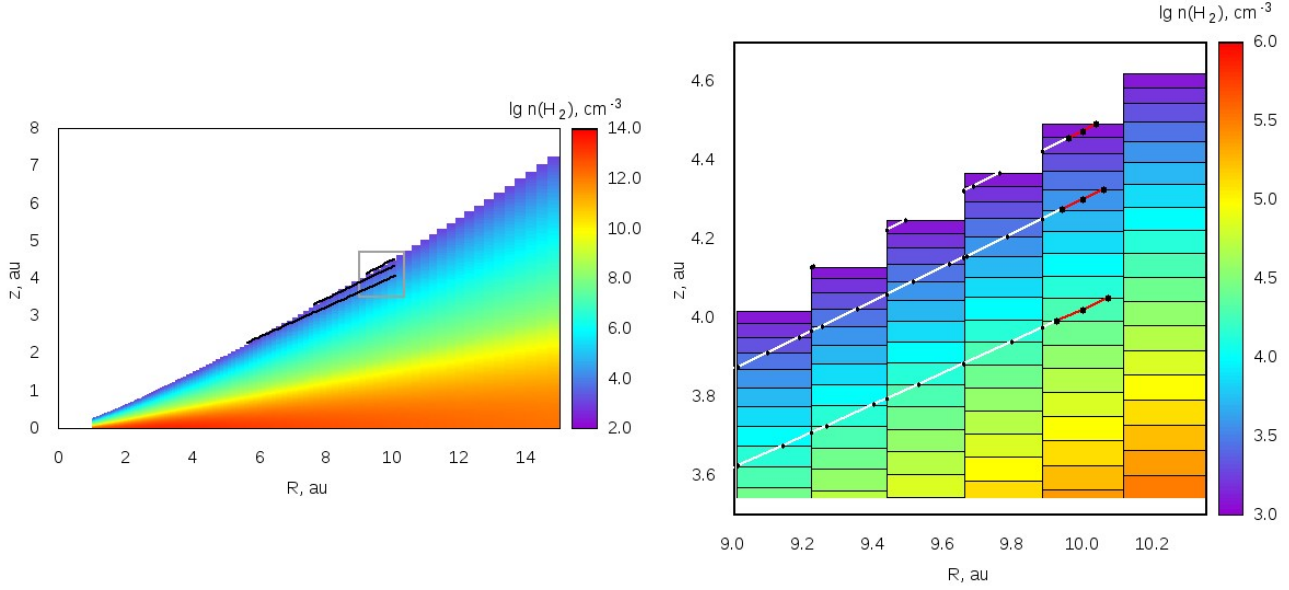


Figure 1. Illustration of the ray tracing on the adopted discrete grid. When integrating the radiation transfer equation along the ray from the star to the current cell, all intersections of the ray with the cell boundaries are found (shown as black dots in the right panel), which is used for accurate calculation of total optical depth. The final segments of rays belonging to the cells in which heating is calculated are highlighted in red.

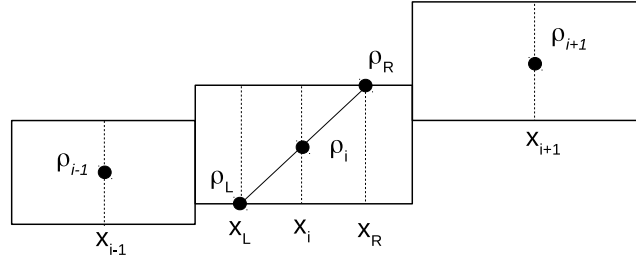


Figure 2. Diagram explaining the calculation of the heating function in the cell.

et al. (2020); Maksimova, Pavlyuchenkov & Tutukov (2020). This model solves radiative transfer problem, taking into account the heating by stellar and interstellar radiation, as well as the diffusion of thermal (infrared) radiation of the disk itself. The vertical disk structure is derived consistently with the temperature calculation. Diffusion of thermal radiation in the model is calculated only in the vertical (z) direction. To model it, we solve system of moment transport equations in the Eddington approximation:

$$c_V \frac{\partial T}{\partial t} = \kappa_P c (E - aT^4) + S \quad (1)$$

$$\frac{\partial E}{\partial t} - \frac{\partial}{\partial z} \left(\frac{c}{3\rho\kappa_R} \frac{\partial E}{\partial z} \right) = -\kappa_P c (E - aT^4), \quad (2)$$

where T is the medium temperature, E is the density of radiation energy, z is the vertical coordinate, ρ is the gas+dust volume density, c_V is the heat capacity of the gas-dust medium, c is the speed of light, a is the radiative constant, κ_P [$\text{cm}^2 \text{g}^{-1}$] is the Planck-averaged absorption coefficient (per unit mass of the gas-dust mixture), κ_R [$\text{cm}^2 \text{g}^{-1}$] is the Rosseland-averaged extinction coefficient (absorption+scattering), and S [$\text{erg s}^{-1} \text{g}^{-1}$] is the heating function (per unit mass of gas-dust medium) by the stellar and interstellar radiation, $S = S^* + S_{\text{bg}}$.

The UV intensity required for the calculation of the heating function S^* is found for each cell by the direct integration of the radiative transfer equation from the star to the considered element throughout the entire disk. This two-dimensional procedure differs from the method described in Vorobyov & Pavlyuchenkov (2017), where the angle between the direction to the star and the surface of the disk was assumed to be constant, and thus the problem there was reduced to one-dimensional one. In the modified method, when integrating transport equation along the ray all intersections with the cell boundaries are identified (see Fig. 1), which is used for exact calculation of the optical depth.

The key aspect in calculating the heating function by stellar radiation within our model is the consideration of the radial density gradient inside the cell. In our model, the heating function s^* [$\text{erg cm}^{-3} \text{s}^{-1}$] by the stellar radiation is calculated as follows:

$$s^* = \rho^* \kappa \frac{L \exp(-\tau)}{4\pi R^2} \left(\frac{1 - \exp(-\Delta\tau)}{\Delta\tau} \right) \quad (3)$$

where L is the luminosity of the star, κ [$\text{cm}^2 \text{g}^{-1}$] is the absorption coefficient for stellar radiation, R is the radial distance from the star to the cell center, τ is the total optical depth along the ray up to the point of entry into the cell, $\Delta\tau = \kappa \rho^* \Delta l$ is the optical

thickness of the cell itself along the ray, Δl is the length of the ray segment inside the cell, $\rho^* = \frac{1}{4}(\rho_L + 2\rho_i + \rho_R)$ is the average density along the ray. For the deriving of the Equation (3) from the formal solution of the radiative transfer equation we assumed that the density along the ray inside the cell changes linearly from ρ_L to ρ_i and from ρ_i to ρ_R , see diagram in Fig. 2. The values ρ_L and ρ_R , in turn, are found using linear density interpolation between the center of the current cell and the centers of adjacent left and right cells:

$$\rho_L = \rho_i + \frac{x_i - x_L}{x_i - x_{i-1}} (\rho_{i-1} - \rho_i) \quad (4)$$

$$\rho_R = \rho_i + \frac{x_R - x_i}{x_{i+1} - x_i} (\rho_{i+1} - \rho_i). \quad (5)$$

Thus, when calculating the heating function, we use the density averaged over neighboring radial cells rather than the central value (which is adopted in the procedure for calculating the vertical disk structure and assumed to be constant inside the cell). In the absence of such (or more precise) averaging, the cell with larger R does not affect cells with smaller R , and as a consequence, there will be no mechanism for the emergence of thermal wave traveling from outside to inside. With accounting for the density interpolation, the potential mechanism for the appearance of irradiation instability is the following. Let us consider two adjacent columns, inner and outer. Let the outer column heats up, so the density ρ_{i+1} in its upper layers increases, because the characteristic scale of the disk height increases. Increased density in the outer cells leads to an increase in the average density ρ^* in adjacent inner cells, which leads to an increase of s^* . Further development of the process depends on the characteristic thermal time scale and geometric effects of the radiation interception by the inner column.

Heating by the interstellar UV radiation is calculated as:

$$S_{bg} = \kappa_{uv} W \sigma T^4 \exp(-\tau) \left(\frac{1 - \exp(-\Delta\tau)}{\Delta\tau} \right), \quad (6)$$

where κ_{uv} is the absorption coefficient for the interstellar radiation, $W = 10^{-14}$, $T_{bg} = 10^4$ K are the dilution and temperature of the interstellar radiation, τ is the optical depth from the surface disk to the current volume element along the vertical direction, $\Delta\tau$ is the optical thickness of the current element, and σ is the Stefan-Boltzmann constant. Heating by the interstellar radiation is included in the model, since it can be comparable to the heating from the star in the outer parts of the disk at the moments of eclipses of the star by the emerging inhomogeneities of disk surface.

The solution of equations (1)–(2) is found using a fully implicit scheme, which is similar to the numerical scheme for solving the quasilinear equation of thermal conductivity with variable coefficients, described in the book Kalitkin (1978). With linearizing equations and using Newton's method, iterations can diverge at a sufficiently large time step. This situation is rare but still occurs. When divergence of the iterative Newton process appears, we split the time step into substeps. The method allows us to calculate thermal evolution in all disk locations, including optically thick regions in which the characteristic times of heating and cooling processes are comparable with dynamic times.

The thermal structure calculation in this model is closely related to the restoration of the vertical disk structure under the assumption of the local hydrostatic equilibrium, which is found from the following equation:

$$\frac{k_B}{\mu_g m_H} \frac{d(\rho T)}{\rho dz} = -\frac{GM_*}{r^3} z, \quad (7)$$

where k_B is the Boltzmann constant, $\mu_g = 2.3$ is the mean molecular weight, m_H is the atomic mass unit, G is the gravitational constant, and M_* is the mass of the star. Note that when restoring the vertical structure, we do not take into account the self-gravity of the disk, which is justified for the disk parameters used in this work. The calculation of the vertical structure makes it possible to obtain complete information about the distribution of the density and temperature in the disk. For solving the equation of hydrostatic equilibrium an implicit method is also used.

The important condition for the effectiveness of these methods is the optimal choice of a spatial grid in the z -direction. The spatial grid should resolve all a priori unknown features of the solution (density and temperature gradients) taking into account significant limitation on the number of cells and large variation of gas density (up to 10 orders of magnitude). We have developed an algorithm for the construction and adaptive modification of such a grid, based on approximate fast solution of the equation of hydrostatic equilibrium. This method of restoring the disk vertical structure with the calculation of radiation transfer has been extensively tested and compared with other methods. In the stationary mode, the temperature distribution is in good consistence with the results of disk structure modeling obtained by other authors. In the non-stationary regime, the characteristic times of arrival to thermal equilibrium correspond to analytical estimates. More details with description of this method can be found in the article by Vorobyov & Pavlyuchenkov (2017).

The model assumes that the only source of opacity is dust, and the temperatures of gas and dust are equal. Dust to gas mass ratio is assumed to be constant throughout the disk and equal to 0.01. A feature of the thermal model is the use of Planck and Rosseland temperature-dependent opacities. These coefficients are taken from Pavlyuchenkov et al. (2020), where they are described in detail.

The main input parameters of the model are the mass and luminosity of the star, which we assume to be solar, as well as the distribution of the surface density, which is chosen by us in the form:

$$\Sigma(R) = \Sigma_0 \left(1 - e^{-\left(\frac{R}{R_0}\right)^p} \right) \left(\frac{R}{R_{au}} \right)^q, \quad (8)$$

where Σ_0 is the surface density near the inner boundary $R_{au}=1$ au, $q = -1$ is the slope of the density distribution, $R_0=3$ au, $p = 8$ is the density distribution smoothing parameters near the inner edge of the disk. The inner and outer boundaries of the disk are equal to 1 and 100 au, respectively. Note that in the absence of smoothing the surface density distribution near the inner disk boundary, the inner cells intercept most of the stellar radiation and strongly influence the structure and evolution of the disk, making it difficult to analyze the surface instability itself. Initial disk state is calculated under the assumption of a constant angle of entry of radiation into the disk within the thermal model Vorobyov & Pavlyuchenkov (2017). The time step is chosen constant and equal to 0.1 yr, which is less than the characteristic thermal time scales at the adopted model parameters. The calculation is carried out on a grid of 200 radial \times 120 vertical cells.

The difference between the presented numerical model and analytical model used in Wu & Lithwick (2021) is the treatment of the detailed two-dimensional structure of the disk. In our case, the heating by the stellar UV radiation is calculated using direct integration of radiation transfer equation, while the intrinsic diffusive thermal radiation is simulated over whole vertical extent.

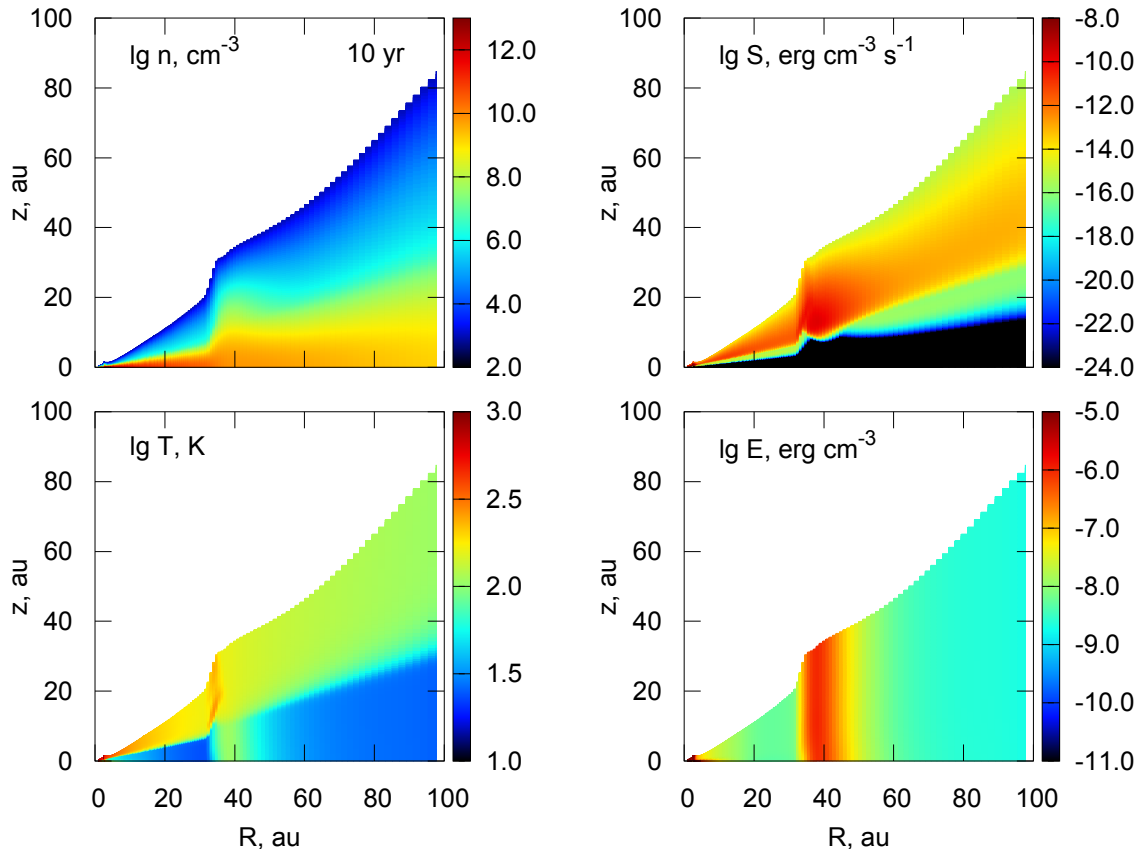


Figure 3. The structure of the protoplanetary disk with $\Sigma_0 = 10^2 \text{ g cm}^{-2}$ at 10 yr after the start of evolution. Shown are the distribution of the logarithm of the gas number density (top left), the logarithm of the temperature (bottom left), the logarithm of the UV heating function (top right), and the logarithm of the IR energy density.

3 RESULTS

Modeling the disk evolution within the framework of the described 1+1D approach shows that perturbations spontaneously arise in the disk, propagating towards the star. The characteristics of these perturbations strongly depend, in particular, on the assumed surface density of the disk. Consider simulation results for a disk with $\Sigma_0 = 10^2 \text{ g cm}^{-2}$ (corresponding to the disk mass $7 \times 10^{-3} M_\odot$). Fig. 3 shows the disk structure (distributions of the gas number density, temperature, UV heating and energy density of IR radiation) at the moment 10 yr after the start disk evolution. In the vicinity of 35 au one can see a bend in the surface geometry, behind which the characteristic scale height of the disk increases. This perturbation propagates inward. Behind the bend, the stellar radiation heating function increases in the disk atmosphere, which is associated with a steeper angle of stellar radiation entry into the disk. The maximum of the heating function in the bend vicinity is associated with the temperature maximum. The temperature is also increased in the disk midplane at some distance behind the bend, which is due to finite time scale for heating of the inner layers by IR radiation of the surface layers. In the vicinity of the perturbed layer the energy density of infrared radiation is enhanced, which also indicates stronger heating of this layer.

The space-time diagram showing the evolution of the midplane temperature is shown in the left panel of Fig. 4. Inward mov-

ing waves stand out well on it, they correspond to maxima moving from right to left with increasing time. Waves extend from the outer edge of the disk to the region of ≈ 3 au, which is transparent to the UV radiation of the star (due to its low density because of the smoothing of the $\Sigma(R)$ distribution). This diagram also includes the distribution of the characteristic thermal time calculated as:

$$t_{\text{therm}} = \frac{3}{8} \frac{c_p \Sigma \tau_{\text{IR}}}{\sigma T_m^3}, \quad (9)$$

where $\tau_{\text{IR}} = \kappa_p \Sigma$ is the optical depth in vertical direction for intrinsic thermal radiation, T_m is the midplane temperature, c_p is the specific heat, and σ is the Stefan–Boltzmann constant. Equation (9) is obtained under assumption that the disk is optically thick to its own thermal radiation, and serves as an estimate for the characteristic heating (or cooling) time scale of the midplane layers to the temperature of T_m . Periodicity of waves of ≈ 3 yr is close to the maximum characteristic thermal time scale ≈ 7 yr, i.e. the perturbed regions of the disk do warm up to the midplane.

The right panel of Fig. 4 shows the evolution of the midplane temperature for a disk model with the same parameters, but without interpolation of the density over the cell in radial direction during the calculation of the heating rate by the stellar radiation, i.e. where $\rho^* = \rho_i$ is assumed, see Equation (3). In this case, several bumps appear in the disk, intercepting the radiation of the star and shading areas behind them. The slow movement of these humps towards the

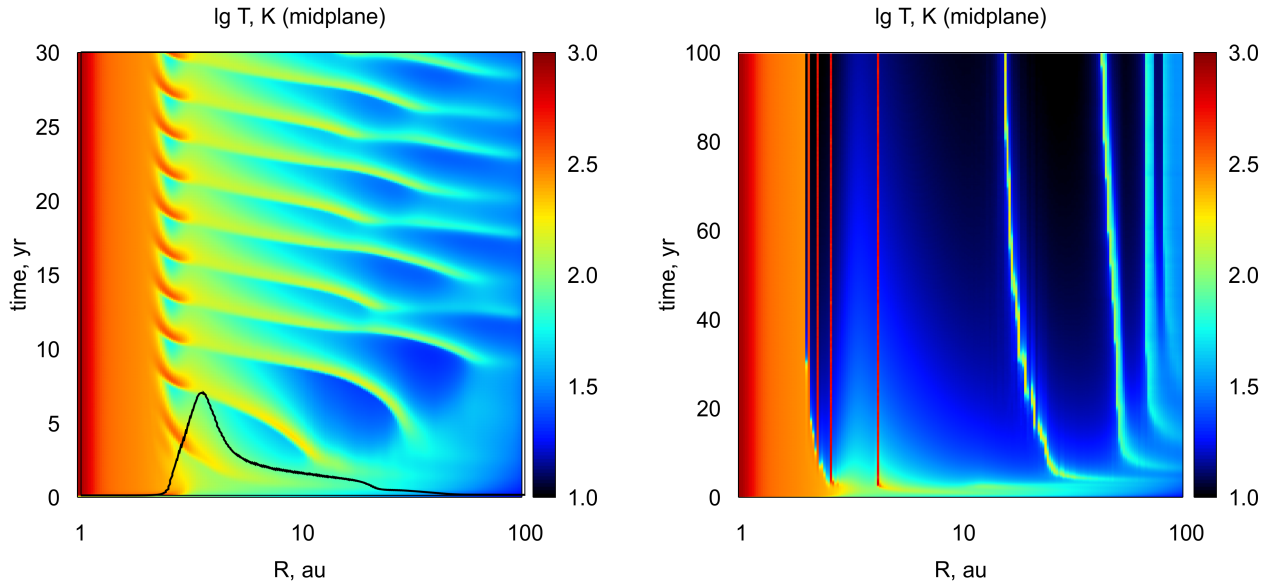


Figure 4. Left panel: evolution of midplane temperature T_m for the disk model with $\Sigma_0 = 10^2 \text{ g cm}^{-2}$. The distance to the star is shown on the horizontal axis, time is along the vertical axis. The black line shows the dependence of the characteristic thermal time scale t_{therm} on the distance for a time moment of 30 yr. Right panel: evolution of T_m for a model without interpolation of density in the radial direction in the calculation of the heating rate by the stellar radiation.

star at the initial stages of the disk evolution is associated with the establishing the self-consistent solution over the thermal time scale. Regular surface waves do not arise in such a model. This simulation shows the importance of using high approximation schemes when integrating the radiative transfer equation in this problem.

Fig. 5 shows the distributions of physical quantities for the model with enhanced surface density, $\Sigma_0 = 10^3 \text{ g cm}^{-2}$, at the moment of 10 yr from the beginning of evolution. The structure of this disk is inhomogeneous. Two perturbations can be distinguished in the energy density distribution of IR radiation: in the vicinity of 10 and 40 au. The morphology of these disturbances generally repeats the pattern described for the previous model. However, unlike the previous model, the heated area in the vicinity of disturbances does not reach the midplane. This can be clearly seen from the top left panel of Fig. 6, which shows evolution of the midplane temperature distribution in the first 20 yr. The waves do not appear in this diagram, with the exception of weak oscillations in vicinity of 3 au. The inward propagating waves, however, are clearly visible on surface temperature distributions (lower left panel of Fig. 6) and temperatures at half surface density up to equator (upper right panel of Fig. 6). Over the considered time interval, the disturbances are generated in the vicinity of 20 au and spread inward in within 3 yr. As they approach the inner boundary of the disk, the propagation velocity of perturbations decreases. The period of passage of these waves is much shorter than the thermal time scale t_{therm} calculated for the entire thickness of the disk. This is evident from the bottom right panel of Fig. 6, where the distribution of thermal time scale for the entire thickness of the disk is plotted. The time t_{therm} is about hundreds of years for the region between 3 and 20 au. On the same panel we show the evolution of midplane temperature of the disk during 1000 yr, i.e. over time comparable with the characteristic thermal time. In this diagram, the waves inside 20 au are also not identified but quasi-periodic perturbations propagating inward from the outer edge of the disk are visible with a occurrence

period ≈ 100 yr. Obviously, the waves in the outer region of the disk are identified on midplane temperature distribution due to the fact that the characteristic thermal times in this region are significantly shorter than in more internal parts, i.e. disk being perturbed on the surface in these regions has time to warm up to the equator.

4 DISCUSSION

The main purpose of this work is to test the possibility of spontaneous excitation of surface thermal waves in protoplanetary disks. To achieve this goal, we updated the previously developed 1+1D disk model with a more accurate (two-dimensional) calculation of the disk heating by the stellar radiation. In the modified model, heating is calculated by integrating the radiative transfer equation along the entire disk taking into account the radial density gradient inside the cell, for which the heating function is calculated. This allows us to account for geometric effects that are of key importance for this task. The simulation results showed that the instability does indeed arise, leading to the emergence of inward moving perturbations. Thus, we confirm the previously obtained by other authors conclusions on possible spontaneous excitation of the surface thermal waves in protoplanetary disks.

In our disk model, we focus on the occurrence of thermal surface waves, as far as feasible “in a pure form” in connection with the fact that there are still questions of their formation. Therefore, many processes essential for disk evolution are not taken into account in this model. In particular, we do not take into account internal viscous heating, which can play an important role in the evolution of the disk, providing an irregular mode of accretion (we studied this effect earlier in Pavlyuchenkov et al. (2020); Maksimova, Pavlyuchenkov & Tutukov (2020)). Neglecting the viscous heating is equivalent to assuming low accretion rate through the disk.

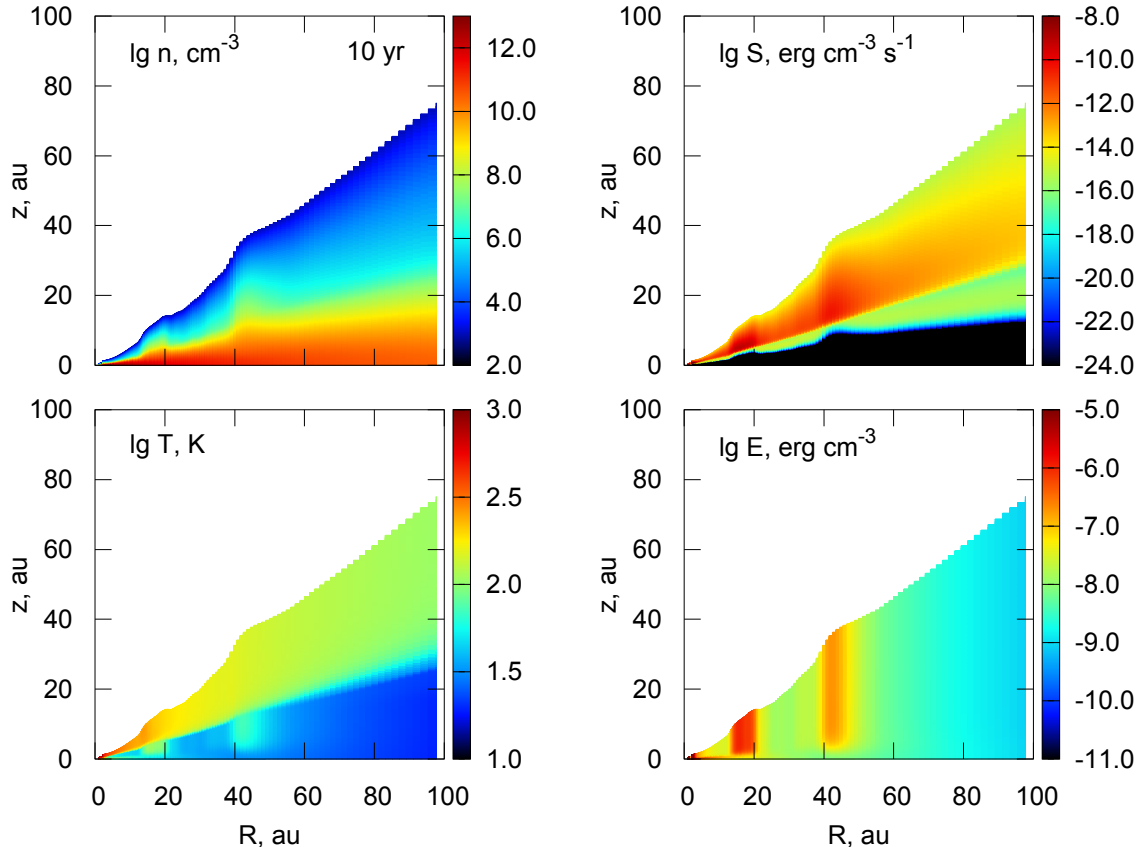


Figure 5. Disk model for $\Sigma_0 = 10^3 \text{ g cm}^{-2}$ at 10 yr after the start of evolution.

Surely, at temperatures of the order of thousands of degrees, the assumption of our model that the opacity is due only to dust is not fulfilled. At such temperatures dust evaporation becomes important, and gas begins to dominate in opacity. At high temperatures other processes become significant, such as the dissociation of hydrogen. In this case, one can expect the appearance of various instabilities in the disk and the complex dynamics associated with them. This is a separate issue requiring detailed study. We note that with our model parameters such high temperatures are obtained only in the most inner ($< 3 \text{ au}$) regions of the disk and do not affect more distant regions, where the thermal waves originate and begin to propagate.

In our model, we also do not take into account dust sedimentation, migration, growth and destruction, which play a critical role in protoplanetary disks. Taking these processes into account can significantly modify or even completely suppress the instability of the disk associated with the effects of self-shadowing. We also note that the mere presence of dust leads to its own instabilities, such as streaming instability (Youdin & Goodman 2005). Streaming instability now becomes very popular for explaining turbulence and formation of planetary embryos. The study of these processes is a separate direction for which complex dynamical models are developed. In this work, we do not consider all these processes, postponing the study of their interaction with the irradiation instability for the future.

A significant difference between our results and the conclu-

sions of the analytical model by Wu & Lithwick (2021) are characteristic timescales for propagation of perturbations. According to the analytical model presented in Wu & Lithwick (2021), characteristic propagation time of perturbations corresponds to the thermal time scale for the entire vertical column of the disk. This result is natural, since in frame of that analytical model, the height of the disk is determined exclusively by the midplane temperature. In our model, the propagation times for optically thick disks turn out to be significantly smaller than the thermal time scale t_{term} . This is explained by the fact that traveling perturbations do not affect the entire thickness of the disk, i.e. wave excitation mechanism can work in the sub-surface layers.

The obtained results indicate the need to study the irradiation instability using more consistent models. Indeed, the 1+1D approach we used is based on several key approximations that can significantly distort the real picture. Such approximations are: 1) the hydrostatic equilibrium in the vertical direction; 2) the absence of the thermal radiation diffusion in the radial direction; 3) the lack of dynamical interaction between disk regions in the radial direction. The influence of these effects on the excitation of surface thermal waves should be explored within the framework of a two-dimensional or three-dimensional hydrodynamic models with a detailed calculation of the radiative transfer. Particular attention in such model should be paid to the treatment of the heating function by the stellar radiation.

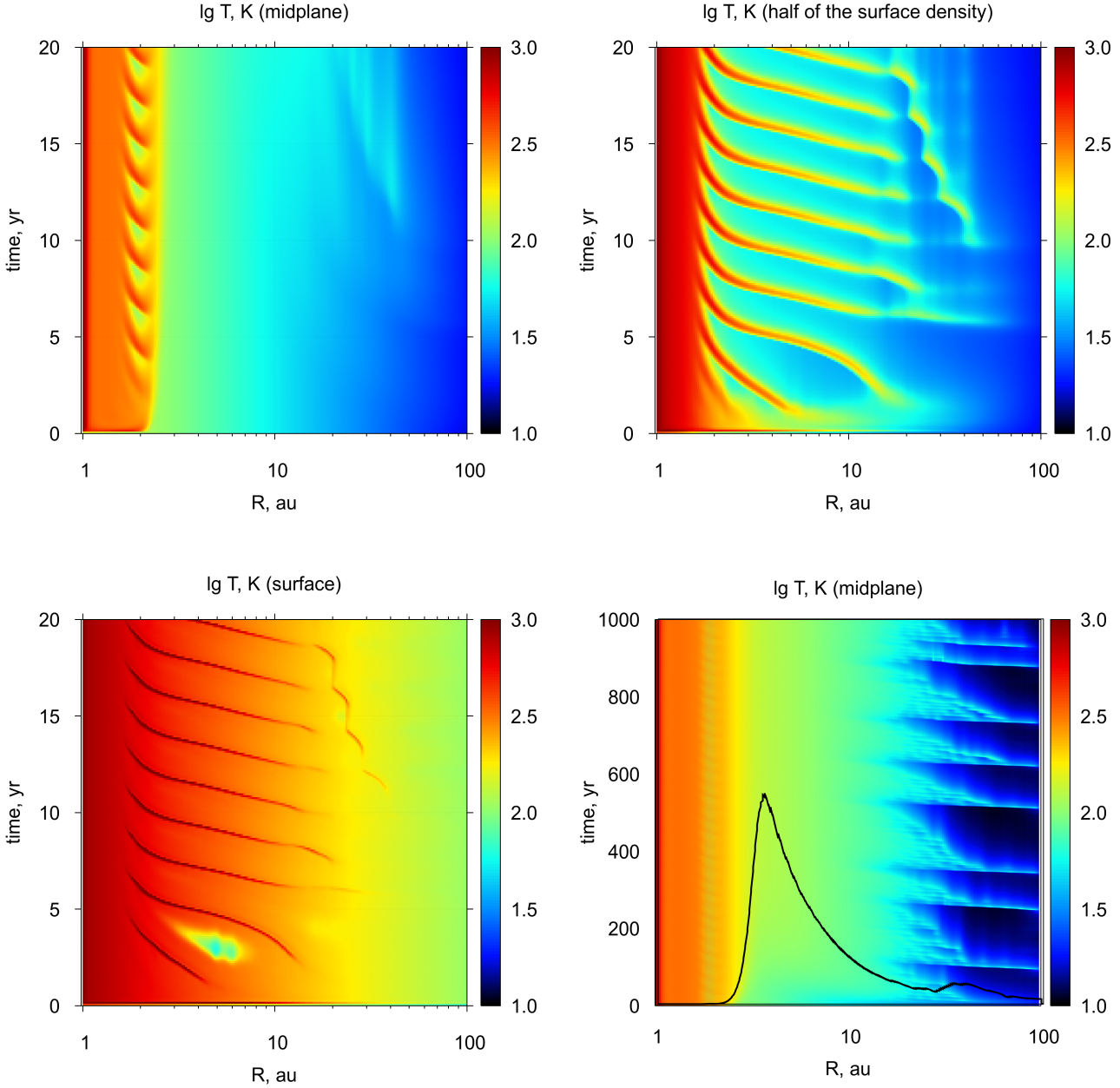


Figure 6. Evolution of temperature distributions for the disk model with $\Sigma_0 = 10^3 \text{ g cm}^{-2}$. Left top panel: midplane temperature for 20 yr. Left bottom panel: disk surface temperature. Top right panel: temperature at half surface density from the upper boundary of the disk to the equator. Right bottom panel: long-term evolution of midplane temperature over 1000 yr. The black curve shows the dependence of the characteristic thermal time t_{therm} on distance.

ACKNOWLEDGMENTS

The authors thank the reviewer for valuable comments and constructive suggestions for improving this article.

FUNDING

The reported study was funded by RFBR according to the research project 20-32-90103. VVA was supported by the Foundation for the Advancement of Theoretical Physics and Mathematics "BASIS" (20-1-2-20-1).

REFERENCES

- ALMA Partnership et al., 2015, *Astrophys. J. L.*, 808, L3
- Andrews S. M., 2020, *Annual Review of Astronomy and Astrophysics*, 58, 483
- Bae J., Zhu Z., Hartmann L., 2017, *ApJ*, 850, 201
- Baruteau C. et al., 2014, in *Protostars and Planets VI*, Beuther H., Klessen R. S., Dullemond C. P., Henning T., eds., p. 667
- D'Alessio P., Cantó J., Hartmann L., Calvet N., Lizano S., 1999, *ApJ*, 511, 896
- Dipierro G., Laibe G., Price D. J., Lodato G., 2016, *Monthly Notices Roy. Astron. Soc.*, 459, L1

- Dong R., Zhu Z., Whitney B., 2015, *ApJ*, 809, 93
Dullemond C. P., 2000, *Astron. and Astrophys.*, 361, L17
Huang J. et al., 2018, *Astrophys. J. L.*, 869, L42
Kalitkin N. N., 1978, *Chislennye metody*. Nauka, Moskva
Maksimova L. A., Pavlyuchenkov Y. N., Tutukov A. V., 2020, *Astronomy Reports*, 64, 815
Pavlyuchenkov Y. N., Tutukov A. V., Maksimova L. A., Vorobyov E. I., 2020, *Astronomy Reports*, 64, 1
Siebenmorgen R., Heymann F., 2012, *Astron. and Astrophys.*, 539, A20
Ueda T., Flock M., Birnstiel T., 2021, *Astrophys. J. L.*, 914, L38
Vorobyov E. I., Pavlyuchenkov Y. N., 2017, *Astron. and Astrophys.*, 606, A5
Watanabe S.-i., Lin D. N. C., 2008, *ApJ*, 672, 1183
Wu Y., Lithwick Y., 2021, *ApJ*, 923, 123
Youdin A. N., Goodman J., 2005, *ApJ*, 620, 459
Zhang S. et al., 2018, *Astrophys. J. L.*, 869, L47